Chiral Phase Transition Temperature in (2 + 1)-Flavor QCD

H.-T. Ding,[1] P. Hegde,[2] O. Kaczmarek,[1,3] F. Karsch,[3,4] Anirban Lahiri,[3] S.-T. Li,[1] Swagato Mukherjee,[4] H. Ohno,[5] P. Petreczky,[4] C. Schmidt,[3] and P. Steinbrecher[4]

(HotQCD Collaboration)

[1]*Key Laboratory of Quark & Lepton Physics (MOE) and Institute of Particle Physics, Central China Normal University, Wuhan 430079, China*
[2]*Center for High Energy Physics, Indian Institute of Science, Bangalore 560012, India*
[3]*Fakultät für Physik, Universität Bielefeld, D-33615 Bielefeld, Germany*
[4]*Physics Department, Brookhaven National Laboratory, Upton, New York 11973, USA*
[5]*Center for Computational Sciences, University of Tsukuba, Tsukuba, Ibaraki 305-8577, Japan*

(Received 14 March 2019; published 8 August 2019)

We present a lattice-QCD-based determination of the chiral phase transition temperature in QCD with two degenerate, massless quarks and a physical strange quark mass using lattice QCD calculations with the highly improved staggered quarks action. We propose and calculate two novel estimators for the chiral transition temperature for several values of the light quark masses, corresponding to Goldstone pion masses in the range of 58 MeV $\lesssim m_\pi \lesssim$ 163 MeV. The chiral phase transition temperature is determined by extrapolating to vanishing pion mass using universal scaling analysis. Finite-volume effects are controlled by extrapolating to the thermodynamic limit using spatial lattice extents in the range of 2.8–4.5 times the inverse of the pion mass. Continuum extrapolations are carried out by using three different values of the lattice cutoff, corresponding to lattices with temporal extents $N_\tau = 6$, 8, and 12. After thermodynamic, continuum, and chiral extrapolations, we find the chiral phase transition temperature $T_c^0 = 132^{+3}_{-6}$ MeV.

DOI: 10.1103/PhysRevLett.123.062002

Introduction.—For physical values of the light up, down, and heavier strange quark masses, strongly interacting matter undergoes a transition from a low-temperature hadronic regime to a high-temperature region that is best described by quark and gluon degrees of freedom. This smooth crossover between the two asymptotic regimes is not a phase transition [1]. It is characterized by a pseudocritical temperature, T_{pc}, that has been determined in several numerical studies of quantum chromodynamics (QCD) [2–4]. A recent determination of T_{pc} extracted from the maximal fluctuations of several chiral observables gave $T_{pc} = (156.5 \pm 1.5)$ MeV [5].

In the chiral limit of $(2 + 1)$-flavor QCD, i.e., where two (degenerate) light quark masses $m_l = (m_u + m_d)/2$ approach zero but the strange quark mass m_s is kept fixed to its physical value, the pseudocritical behavior is expected to give rise to a "true" chiral phase transition [6,7]. The chiral phase transition temperature itself is expected to set an upper bound on the temperature at a possible critical point at nonzero baryon chemical potential [8,9], which is intensively searched for in heavy ion collision experiments. Whether this chiral phase transition is first or second order may depend crucially on the temperature dependence of the chiral anomaly [7]. In the latter case, critical behavior generally is expected to be controlled by the 3D $O(4)$ universality class, although a larger 3D universality class [10,11] may become of relevance in case the axial anomaly also gets restored effectively at T_c^0. If the chiral phase transition is first order, then a second-order phase transition, belonging to the 3D $Z(2)$ universality class, would occur for $m_l^c > 0$. When decreasing the light to strange quark mass ratio, $H = m_l/m_s$, towards zero, this would give rise to diverging susceptibilities already for some critical mass ratio $H_c = m_l^c/m_s > 0$. The analysis presented here leads to a determination of the critical temperature $T_c^{H_c}$. However, as we do not have any evidence for $H_c \neq 0$, we de facto present a determination of the chiral phase transition temperature T_c^0.

Although T_c^0 appears as a fit parameter in all finite-temperature scaling studies of the chiral transition in QCD [3,12,13], so far no lattice QCD calculation has carried out a systematic analysis of T_c^0 by controlling thermodynamic, continuum, and chiral limits. Here, we will present a first

lattice-QCD-based determination of T_c^0 in $(2+1)$-flavor QCD with controlled thermodynamic, continuum, and chiral extrapolations. QCD-inspired model calculations [14,15] suggest that T_c^0 might be even lower (by 20–30 MeV) than T_{pc}. To mitigate this potentially large m_l dependence of T_{pc} while approaching $m_l \to 0$, we propose two novel estimators of the pseudocritical temperature having only mild dependence on m_l, leading to well-controlled chiral extrapolation.

Chiral observables.—At low temperatures, chiral symmetry is spontaneously broken in QCD. An order parameter for the restoration of this symmetry at high temperature is the chiral condensate, which is obtained as the derivative of the partition function, $Z(T,V,m_u,m_d,m_s)$, with respect to one of the quark masses, m_f,

$$\langle\bar{\psi}\psi\rangle_f = \frac{T}{V}\frac{\partial \ln Z(T,V,m_u,m_d,m_s)}{\partial m_f}. \tag{1}$$

The light quark chiral condensate, $\langle\bar{\psi}\psi\rangle_l = (\langle\bar{\psi}\psi\rangle_u + \langle\bar{\psi}\psi\rangle_d)/2$, is an order parameter for the chiral phase transition that occurs in the limit $m_l \to 0$. For nonvanishing m_l, this order parameter requires additive and multiplicative renormalization. We take care of this by introducing a combination of the light and strange quark chiral condensates,

$$M = 2(m_s\langle\bar{\psi}\psi\rangle_l - m_l\langle\bar{\psi}\psi\rangle_s)/f_K^4, \tag{2}$$

where the kaon decay constant, $f_K = 156.1(9)/\sqrt{2}$ MeV, for physical values of the degenerate light and strange quark mass, is used as a normalization constant to define a dimensionless order parameter M. The order parameter M is free of UV divergences linear in the quark masses m [3] but may still receive divergent contributions proportional to $m^3\ln(m)$, which we neglect here. The derivative of M with respect to the light quark masses gives the chiral susceptibility,

$$\begin{aligned}\chi_M &= m_s(\partial_{m_u} + \partial_{m_d})M|_{m_u=m_d} \\ &= m_s(m_s\chi_l - 2\langle\bar{\psi}\psi\rangle_s - 4m_l\chi_{su})/f_K^4,\end{aligned} \tag{3}$$

with $\chi_{fg} = \partial_{m_f}\langle\bar{\psi}\psi\rangle_g$ and $\chi_l = 2(\chi_{uu} + \chi_{ud})$.

When approaching the chiral limit, one also needs to control the thermodynamic limit, $V \to \infty$. In the vicinity of a second-order phase transition, M and χ_M are given in terms of the universal finite-size scaling functions $f_G(z,z_L)$ and $f_\chi(z,z_L)$, which depend on the scaling variables $z = t/h^{1/\beta\delta}$ and $z_L = l_0/(Lh^{\nu/\beta\delta})$. Here $t = (T - T_c^0)/(t_0T_c^0)$ denotes the reduced temperature; $h = H/h_0$ is the symmetry-breaking field; and L/l_0 parametrizes the finite size of the system, $L \equiv V^{1/3}$. These scaling variables are expressed in terms of nonuniversal parameters, t_0, h_0, l_0.

While the universal scaling functions control the behavior of M and χ_M close to a critical point at $(z,z_L) = (0,0)$, they also receive contributions from corrections to scaling and regular terms [16,17], which we represent by a function $f_{\rm sub}(T,H,L)$. With this, we may write

$$\begin{aligned}M &= h^{1/\delta}f_G(z,z_L) + f_{\rm sub}(T,H,L), \\ \chi_M &= h_0^{-1}h^{1/\delta-1}f_\chi(z,z_L) + \tilde{f}_{\rm sub}(T,H,L).\end{aligned} \tag{4}$$

As far as is needed for the analysis, we will specify contributions arising from $f_{\rm sub}(T,H,L)$ later.

Close to the thermodynamic limit, $f_\chi(z,z_L)$ has a pronounced peak, which often is used to define a pseudocritical temperature T_p. In the scaling regime, this peak is located at some $z = z_p(z_L)$, which defines T_p,

$$T_p(H,L) = T_c^0\left(1 + \frac{z_p(z_L)}{z_0}H^{1/\beta\delta}\right) + \text{subleading}, \tag{5}$$

with $z_0 = h_0^{1/\beta\delta}/t_0$. While the first term describes the universal quark mass dependence of T_p, corrections may arise from corrections to scaling and regular terms, shifting the peak location of the chiral susceptibilities.

When approaching the chiral limit, depending on the magnitude of $z_p/z_0 \equiv z_p(0)/z_0$, $T_p(H,L)$ may change significantly with H. In the potentially large temperature interval between T_c^0 and $T_p(H,L)$, regular contributions, arising from $f_{\rm sub}(T,H,L)$, may also be large, and during the $H \to 0$ extrapolation several nonuniversal parameters may be needed to account for contributions from $f_{\rm sub}(T,H,L)$. It is thus advantageous to determine T_c^0 using observables defined close to $z \simeq 0$. While $T_p(H,L)$, defined through such observables for small $H > 0$, will have milder H dependence, the determination of $T_c^0 = T_p(H \to 0, L \to \infty)$ will be well controlled.

We will consider here two estimators for T_c^0, defined at or close to $z = 0$. We determine temperatures T_δ and T_{60} by demanding

$$\frac{H\chi_M(T_\delta,H,L)}{M(T_\delta,H,L)} = \frac{1}{\delta}, \tag{6}$$

$$\chi_M(T_{60},H) = 0.6\chi_M^{\max}. \tag{7}$$

Equation (6) has already been introduced in Ref. [18] as a tool to analyze the chiral transition in QCD, and it is understood that T_{60} is determined at a temperature on the left of the peak $\chi_M^{\max}$, i.e., $T_{60} < T_p$. These relations define pseudocritical temperatures, T_X, which are close to T_c^0 already for nonzero H and L^{-1}. They converge to the chiral phase transition temperature T_c^0 in the thermodynamic and chiral limits. For nonzero L^{-1}, Eqs. (6) and (7) involve scaling variables $z_X(z_L)$ which approach or are close to zero in the limit $L^{-1} \to 0$, i.e., $z_\delta \equiv z_\delta(0) = 0$ and $z_{60} \equiv z_{60}(0) \simeq 0$. Some values for z_{60}, for several universality classes, are given in Table I, and the relevant scaling functions, obtained in the thermodynamic limit $z_L = 0$, are shown in Fig. 1.

TABLE I. The critical exponent δ, the location of the peak z_p, and the position of 60% of the peak value z_{60} of the scaling functions $f_\chi(z)$ for different 3D universality classes [17,19,20]. Also given are $f_G(z_p)$, $f_\chi(z_p)$, and $r_\chi(0) = f_\chi(0)/f_\chi(z_p)$.

	δ	z_p	z_{60}	$f_G(z_p)$	$f_\chi(z_p)$	$r_\chi(0)$
$Z(2)$	4.805	2.00(5)	0.10(1)	0.548(10)	0.3629(1)	0.573(1)
$O(2)$	4.780	1.58(4)	−0.005(9)	0.550(10)	0.3489(1)	0.600(1)
$O(4)$	4.824	1.37(3)	−0.013(7)	0.532(10)	0.3430(1)	0.604(1)

Ignoring possible contributions from corrections to scaling, and keeping in $f_{\rm sub}$ only the leading T-independent, infinite-volume regular contribution proportional to H, we then find for the pseudocritical temperatures

$$T_X(H,L) = T_c^0\left(1 + \left(\frac{z_X(z_L)}{z_0}\right)H^{1/\beta\delta}\right) + c_X H^{1-1/\delta+1/\beta\delta}, \qquad X = \delta, 60. \quad (8)$$

The universal functions, $z_X(z_L)$, may directly be determined from the ratio of scaling functions, $f_\chi(z_\delta, z_L)/f_G(z_\delta, z_L) = 1/\delta$ and $f_\chi(z_{60}, z_L)/f_\chi(z_p, z_L) = 0.6$, respectively. The finite-size scaling functions $f_G(z, z_L)$, $f_\chi(z, z_L)$ have been determined for the 3D, $O(4)$ universality class in Ref. [21].

We will present here results on T_δ and T_{60} obtained in lattice QCD calculations [22]. We have calculated the chiral order parameter M and the chiral susceptibility χ_M [Eqs. (2) and (3)] in $(2+1)$-flavor QCD with degenerate up and down quark masses ($m_u = m_d$). For our lattice QCD calculations, performed with the highly improved staggered quark (HISQ) action [23] in the fermion sector and the Symanzik improved gluon action, the strange quark mass has been tuned to its physical value [24], and the light quark mass has been varied in a range $m_l \in [m_s/160 : m_s/20]$ corresponding to Goldstone pion masses in the range $58\ {\rm MeV} \lesssim m_\pi \lesssim 163\ {\rm MeV}$. At each temperature, we performed calculations on lattices of size $N_\sigma^3 N_\tau$ for three different values of the lattice cutoff, $aT = 1/N_\tau$, with $N_\tau = 6$, 8, and 12. In the HISQ discretization scheme, so-called taste symmetry violations give rise to a distortion of the light pseudoscalar (pion) meson masses. These discretization effects are commonly expressed in terms of a root-mean-square (rms) pion mass which approaches the Goldstone pion mass in the continuum limit. For our computational setup and the three different values of the lattice cutoff, this has been discussed in Ref. [3]. For lattice spacings corresponding to $N_\tau = 6$, 8, and 12, one finds for physical values of the quark masses $M_{\rm rms} = 400$, 300, and 200 MeV, respectively. The spatial lattice extent, $N_\sigma = L/a$, has been varied in the range $4 \le N_\sigma/N_\tau \le 8$. For each N_τ, we analyzed the volume dependence of M and χ_M in order to perform controlled infinite-volume extrapolations.

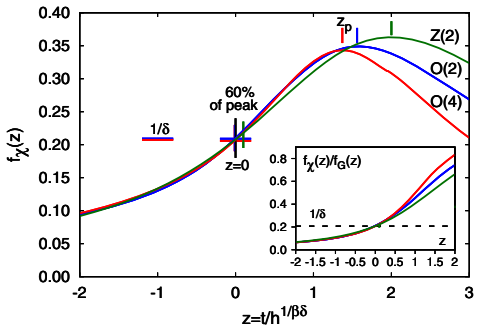

FIG. 1. Scaling functions for the 3D $Z(2)$, $O(2)$, and $O(4)$ universality classes. The position z_p of the peak of the scaling functions (vertical lines) and the position z_{60} where the scaling function attains 60% of its maximal value (crosses) are also given in Table I. Lines close to $z = -1$ show $1/\delta$ for these three universality classes, which agree to within better than 1%. The inset shows the ratio of scaling functions, $f_\chi(z)/f_G(z)$, used in determinations of the chiral phase transition temperature.

Results.—In Fig. 2 (left), we show results for χ_M on lattices with temporal extent $N_\tau = 8$ for five different values of the quark mass ratio, $H = m_l/m_s$, and the largest lattice available for each H. The increase of the peak height, $\chi_M^{\rm max}$, with decreasing H is apparent. This rise is consistent with the expected behavior, $\chi_M^{\rm max} \sim H^{1/\delta-1} + {\rm const.}$, with $\delta \simeq 4.8$; however, a precise determination of δ is not yet possible with the current data.

In Fig. 2 (right), we show the volume dependence of χ_M for $H = 1/80$ on lattices with temporal extent $N_\tau = 8$ and for $N_\sigma/N_\tau = 4$, 5, and 7. Similar results have also been obtained for $N_\tau = 6$ and 12. We note that $\chi_M^{\rm max}$ decreases slightly with increasing volume, contrary to what one would expect to find at or close to a first- or second-order phase transition. Our current results, thus, are consistent with a continuous phase transition at $H_c = 0$.

Using results for χ_M and M, we constructed the ratios $H\chi_M/M$ for different lattice sizes and several values of the quark masses. This is shown in Fig. 3 (left) for the lightest quark masses used on the $N_\tau = 12$ lattices, $H = 1/80$. The intercepts with the horizontal line at $1/\delta$ define $T_\delta(H,L)$. For $H = 1/80$ and each of the three temporal lattice sizes, we have results for three different volumes on which we can extrapolate $T_\delta(H,L)$ to the infinite-volume limit. We performed such extrapolations using (i) the $O(4)$ ansatz given in Eq. (8), as well as (ii) an extrapolation in $1/V$. The latter is appropriate for large L, if the volume dependence predominantly arises from regular terms, and the former is appropriate close to or in the continuum limit, if the singular part dominates the partition function. In the former case, we use the approximation $z_\delta(z_L) \sim z_L^{5.7}$, which parametrizes well the finite-size dependence of T_δ in the scaling regime [21]. The resulting fits are shown in Fig. 3 (middle). We note that results for fixed H tend to approach the infinite-volume limit more rapidly than $1/V$, which is in

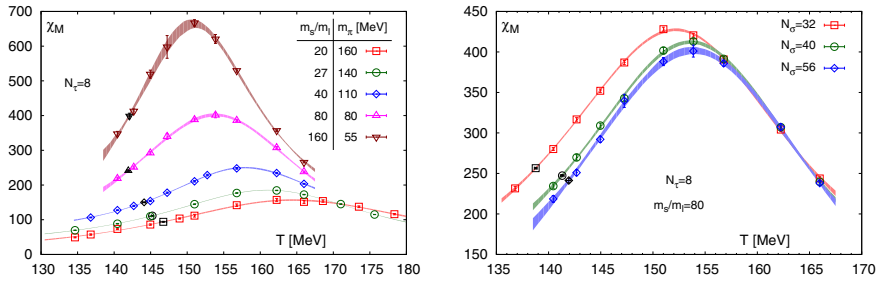

FIG. 2. Quark mass (left) and volume (right) dependence of the chiral susceptibility on lattices with temporal extent $N_\tau = 8$. The left-hand figure shows results for several values of the quark masses. The spatial lattice extent N_σ is increased as the light quark mass decreases: $N_\sigma = 32$ ($H^{-1} = 20, 27$), 40 ($H^{-1} = 40$), 56 ($H^{-1} = 80, 160$). The right-hand figure shows results for three different spatial lattice sizes at $H = 1/80$. Black symbols mark the points corresponding to 60% of the peak height.

accordance with the behavior expected from the ratio of finite-size scaling functions. The resulting continuum limit extrapolations in $1/N_\tau^2$ based on data for (i) all three N_τ values, as well as (ii) $N_\tau = 8$ and 12 only, are shown as horizontal bars in this figure. An analogous analysis is performed for $H = 1/40$. Finally, we extrapolate the continuum results for $T_\delta(H, \infty)$ with $H = 1/40$ and $1/80$ to the chiral limit, using Eq. (8) with $z_\delta(0) = 0$. Results obtained from these extrapolation chains, which involve either a $1/V$ or $O(4)$ ansatz for the infinite-volume extrapolation, as well as continuum limit extrapolations performed on two different datasets, lead to chiral transition temperatures T_c^0 in the range (128–135) MeV. The resulting values for T_c^0 are summarized in Fig. 4.

As the fits shown in Fig. 3 (middle) suggest that the $O(4)$ scaling ansatz is appropriate for the analysis of finite-volume effects already at nonzero values of the cutoff, we can attempt a combined analysis of all data available for different light quark masses and volumes at fixed N_τ. This utilizes the quark mass dependence of finite-size corrections, expressed in terms of z_L, and thus it intertwines continuum and chiral limit extrapolations. Using the scaling ansatz given in Eq. (8), it also allows us to account for the contribution of a regular term in a single fit. Fits for fixed N_τ based on this ansatz, using data for all available lattice sizes and $H \leq 1/27$, are shown in Fig. 3 (right). For each N_τ, the fit yields results for $T_\delta(H, L)$ at arbitrary H. Some bands for $H = 1/40$ and $1/80$ are shown in the figure. As can be seen, for $H = 1/80$, these bands compare well with the fits shown in Fig. 3 (middle). For each N_τ, an arrow shows the corresponding chiral limit result, $T_\delta(0, \infty)$. We extrapolated these chiral limit results to the continuum limit and estimated systematic errors again by including or leaving out data for $N_\tau = 6$. The resulting T_c^0 values, shown in Fig. 4, are in complete agreement with the corresponding numbers obtained by first taking the continuum limit and then taking the chiral limit. Within the current accuracy, these two limits are interchangeable.

Similarly, we analyzed results for T_{60} on all datasets using the same analysis strategy as for T_δ. As can be seen in Fig. 4, we find for each extrapolation ansatz that the resulting values for T_c^0 agree to within better than 1% accuracy with the corresponding values for T_δ. This corroborates that the chiral susceptibilities used for this analysis reflect basic features of the $O(4)$ scaling functions.

Performing continuum extrapolations by either including or discarding results obtained on the coarsest ($N_\tau = 6$) lattices leads to a systematic shift of about 2–3 MeV in the estimates for T_c^0. This is reflected in the displacement of the two bands in Fig. 4, which show averages for T_c^0 obtained

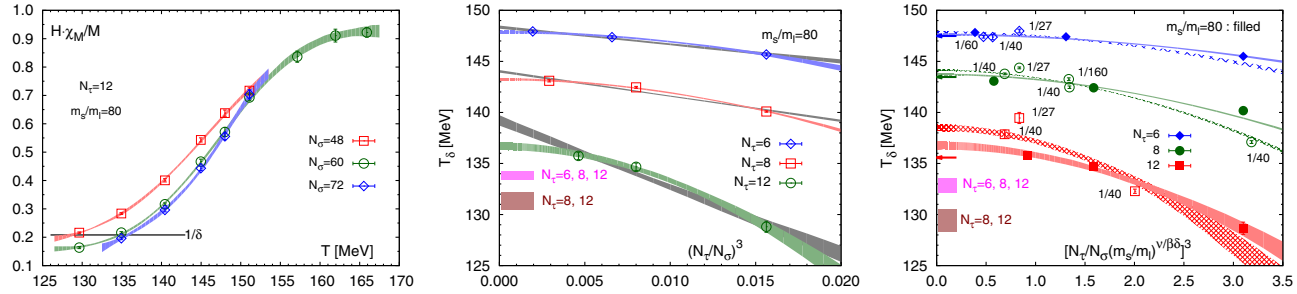

FIG. 3. *Left*: The ratio $H\chi_M/M$ versus temperature for $N_\tau = 12$, $m_l/m_s = 1/80$ and different spatial volumes. *Middle*: Infinite-volume extrapolations based on an $O(4)$ finite-size scaling ansatz (colored bands) and fits linear in $1/V$ (gray bands). Horizontal bars show the continuum extrapolated results for $H = 1/80$. *Right*: Finite-size scaling fits for T_δ based on all data for $H \leq 1/27$ and all available volumes. Arrows show chiral limit results at fixed N_τ, and horizontal bars show the continuum extrapolated results for $H = 0$.

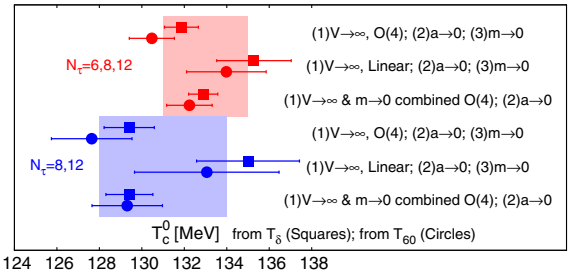

FIG. 4. Summary of fit results. For details, see text.

with our different extrapolation *Ansätze*. Averaging separately over results for T_δ and T_{60} obtained with both continuum extrapolation procedures and including this systematic effect, we find for the chiral phase transition temperature

$$T_c^0 = 132^{+3}_{-6}\ \mathrm{MeV}. \tag{9}$$

Conclusions.—Based on two novel estimators, we have determined the chiral phase transition temperature in QCD with two massless light quarks and a physical strange quark. Equation (9) gives our thermodynamic-, continuum-, and chiral-extrapolated result for the chiral phase transition temperature, which is about 25 MeV smaller than the pseudocritical (crossover) temperature T_{pc} for physical values of the light and strange quark masses [5]. Lattice QCD calculations presented here were carried out using the so-called "rooted" staggered fermion formulation. There are ample theoretical and numerical evidences (for a review, see Ref. [25]) that once the proper order of the limits—first continuum, and then chiral—is followed, this formulation produces correct physical results [26,27]. In the present calculations, we followed the proper order of the limits. However, we also checked that the quoted value T_c^0 remained unchanged, within our numerical accuracies, even when joint chiral and continuum limits were carried out. Notwithstanding such reassuring checks, in the future it will be important to carry out similar lattice QCD calculations using other fermion actions. The two estimators proposed in the current Letter will also be useful in such calculations.

This work was supported in part by the Deutsche Forschungsgemeinschaft (DFG) through Grant No. 315477589-TRR 211, by Grants No. 05P15PBCAA and No. 05P18PBCA1 of the German Bundesministerium für Bildung und Forschung, and by the National Natural Science Foundation of China under Grants No. 11775096 and No. 11535012. Furthermore, this work was supported by Contract No. DE-SC0012704 with the U.S. Department of Energy, by the Scientific Discovery through Advanced Computing (SciDAC) program funded by the U.S. Department of Energy, by the Office of Science, Advanced Scientific Computing Research and Nuclear Physics, by the DOE Office of Nuclear Physics funded BEST topical collaboration, and by a Early Career Research Award of the Science and Engineering Research Board of the Government of India. Numerical calculations have been made possible through PRACE grants at CSCS, Switzerland, and at CINECA, Italy as well as grants at the Gauss Centre for Supercomputing and NIC-Jülich, Germany. These grants provided access to resources on Piz Daint at CSCS and Marconi at CINECA, as well as on JUQUEEN and JUWELS at NIC. Additional calculations have been performed on GPU clusters of USQCD, at Bielefeld University, the PC^2 Paderborn University, and the Nuclear Science Computing Center at Central China Normal University, Wuhan, China. Some datasets have also partly been produced at the TianHe II Supercomputing Center in Guangzhou.

[1] For a recent review, see H. T. Ding, F. Karsch, and S. Mukherjee, Int. J. Mod. Phys. E **24**, 1530007 (2015).
[2] Y. Aoki, S. Borsanyi, S. Durr, Z. Fodor, S. D. Katz, S. Krieg, and K. K. Szabo, J. High Energy Phys. 06 (2009) 088.
[3] A. Bazavov *et al.*, Phys. Rev. D **85**, 054503 (2012).
[4] C. Bonati, M. D'Elia, M. Mariti, M. Mesiti, F. Negro, and F. Sanfilippo, Phys. Rev. D **92**, 054503 (2015).
[5] A. Bazavov *et al.* (HotQCD Collaboration), Phys. Lett. B **795**, 15 (2019).
[6] J. B. Kogut, M. Stone, H. W. Wyld, J. Shigemitsu, S. H. Shenker, and D. K. Sinclair, Phys. Rev. Lett. **48**, 1140 (1982).
[7] R. D. Pisarski and F. Wilczek, Phys. Rev. D **29**, 338 (1984).
[8] M. A. Halasz, A. D. Jackson, R. E. Shrock, M. A. Stephanov, and J. J. M. Verbaarschot, Phys. Rev. D **58**, 096007 (1998).
[9] F. Karsch, arXiv:1905.03936.
[10] M. Grahl and D. H. Rischke, Phys. Rev. D **88**, 056014 (2013).
[11] A. Pelissetto and E. Vicari, Phys. Rev. D **88**, 105018 (2013).
[12] S. Ejiri, F. Karsch, E. Laermann, C. Miao, S. Mukherjee, P. Petreczky, C. Schmidt, W. Soeldner, and W. Unger, Phys. Rev. D **80**, 094505 (2009).
[13] F. Burger, E. M. Ilgenfritz, M. P. Lombardo, and A. Trunin, Phys. Rev. D **98**, 094501 (2018).
[14] J. Berges, D. U. Jungnickel, and C. Wetterich, Phys. Rev. D **59**, 034010 (1999).
[15] J. Braun, B. Klein, H.-J. Pirner, and A. H. Rezaeian, Phys. Rev. D **73**, 074010 (2006).
[16] M. Hasenbusch, J. Phys. A **34**, 8221 (2001).
[17] J. Engels, S. Holtmann, T. Mendes, and T. Schulze, Phys. Lett. B **492**, 219 (2000).
[18] F. Karsch and E. Laermann, Phys. Rev. D **50**, 6954 (1994).
[19] J. Engels, L. Fromme, and M. Seniuch, Nucl. Phys. **B655**, 277 (2003).
[20] J. Engels and F. Karsch, Phys. Rev. D **85**, 094506 (2012).

[21] J. Engels and F. Karsch, Phys. Rev. D **90**, 014501 (2014).
[22] We reported on preliminary results from this work in H.-T. Ding, P. Hegde, F. Karsch, A. Lahiri, S.-T. Li, S. Mukherjee, and P. Petreczky, Nucl. Phys. **A982**, 211 (2019).
[23] E. Follana, Q. Mason, C. Davies, K. Hornbostel, G. P. Lepage, J. Shigemitsu, H. Trottier, and K. Wong (HPQCD and UKQCD Collaborations), Phys. Rev. D **75**, 054502 (2007).
[24] For details on the tuning of quark masses, the determination of lines of constant physics and scale setting used in our calculations, see A. Bazavov *et al.* (HotQCD Collaboration), Phys. Rev. D **90**, 094503 (2014).
[25] S. R. Sharpe, Proc. Sci., LAT2006 (**2006**) 022.
[26] C. Bernard, M. Golterman, Y. Shamir, and S. R. Sharpe, Phys. Lett. B **649**, 235 (2007).
[27] C. Bernard, Phys. Rev. D **71**, 094020 (2005).
[28] See Supplemental Material at http://link.aps.org/supplemental/10.1103/PhysRevLett.123.062002 for a table summarizing values of M and χ_M used in the current Letter.